Speed Control Applying Hysteresis Current Combining Sine Pulse Width Modulation for Induction Motor Drive

Minh TRAN[1], *Cuong Dinh TRAN*[2,*], *Bach Hoang DINH*[2], *Tai Thanh PHAN*[3], *Trang Huynh Cong NGUYEN*[3], *Huy Truong NGUYEN*[3], *Giang Thi Tuyet LAI*[3], *Huy Xuan PHAN*[4]

[1]Optoelectronics Research Group, Faculty of Electrical and Electronics Engineering, Ton Duc Thang University, Ho Chi Minh City, Vietnam
[2]Power System Optimization Research Group, Faculty of Electrical and Electronics Engineering, Ton Duc Thang University, Ho Chi Minh City, Vietnam.
[3]Faculty of Electrical and Electronics Engineering, Ton Duc Thang University, Ho Chi Minh City, Vietnam.
[4]Long An Power Company, 168 Tuyen Tranh, Ward. 4, Tan An City, Long An Province, Vietnam.

*Corresponding Author: Cuong Dinh TRAN (Email: trandinhcuong@tdtu.edu.vn)
(Received: 4-Oct-2021; accepted: 7-Feb-2022; published: 31-Mar-2022)
DOI: http://dx.doi.org/10.55579/jaec.202261.348

Abstract. *An enhanced technique combining hysteresis current (HC) and sine pulse width modulation (SPWM) for generating the switching pulse to the inverter is proposed for speed control based on a rotor field-oriented control (RFOC) strategy in the induction motor drive. HC method is a simple and robust control method, it has a fast response in speed control, but the rotor speed and the stator current have high ripple. SPWM method, a popular method in triangular carrier wave modulation methods, has high precision in controlling the speed and torque of the motor; however, the high overshoot of the speed response in the transient phase is the weakness of this method. In this paper, a combined method of the above two methods, called hysteresis current-sine pulse width modulation (HCSPWM), is proposed for motor speed control. The simulations are implemented at various speed ranges in MatLab/Simulink environment. The simulation results have proved that the proposed method has a lower overshoot than the SPWM method in the transient-state and a lower ripple than the HC method in the steady-state in the same operating condition.*

Keywords

Field-oriented control, hysteresis current controller, sine-pulse width modulation, speed control.

Nomenclature

u_{Sx}, u_{Sy}	Stator voltage components in $[x, y]$ system
i_{Sx}, i_{Sy}	Flux and Torque current components
i_m	Magnetizing current
R_S, R_R	Stator and rotor resistances
L_S, L_R	Stator and rotor inductances
L_m	Magnetizing inductances
T_R	Rotor time constant
ω_m, ω_{en}	Mechanical angular speed
p	Pole pair number
ψ_R, γ	Rotor flux and Rotor flux angle

1. Introduction

Once known for the outstanding performance in constant-speed applications, the three-phase induction motor drive (IMD) has overcome the problems of complex control structures to widen the application range in speed control [1]. The robust development of power electronics technology has created flexible Voltage source inverters in supplying electric motors. Correspondingly, modern control algorithms have been focused on recent research to achieve high control efficiency in IMD systems.

In speed control applications where high accuracy is not required, the group of Scalar control methods is a preferred choice [2]. The principle of the Scalar control method is to adjust the voltage and frequency so that they are constant during operation [3, 4]. Typical scalar control systems do not need feedback sensors, thus reducing the cost of the control system [5, 6]. However, IMD applying a scalar control system has a low-speed control response and cannot operate in low-speed areas [7].

Field-oriented control (FOC), a typical method of the vector control group, is applied to high-performance speed control applications [8, 9]. FOC uses a current space vector separation technique to control flux and torque independently, similar to a separately excited DC motor [10, 11]. A $[x, y]$ rotating coordinate system with the x-axis matching to the rotor flux vector is used in the FOC method [12]. The stator current vector is decoupled to two perpendicular components, "i_{Sx}, i_{Sy}," as shown in Fig. 1 [13]. The rotor flux is maintained constant by controlling the "i_{Sx}" component, and the "i_{Sy}" component adjusts the motor torque to achieve the demanded speed [14, 15].

The FOC method's IMD system requires current sensors and a speed sensor for feedback signals to the FOC unit. The FOC unit will generate the demand signals, which be modulated into inverter switching pulses. Finally, the switching pulses will control the power-inverter to provide the voltage to the IMD. Depending on the FOC output demand signal type, we will have different switching pulse modulation methods. If output demand signals are the current signals,

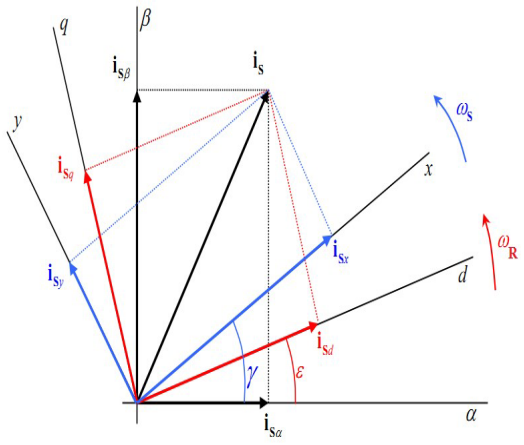

Fig. 1: Current vector diagram of FOC scheme.

the hysteresis current (HC) control method can be used to generate switching pulses. The sine pulse width modulation (SPWM) method can be applied if the output is the demand voltage signals.

In typical HC methods, the inverter switching pulses are resulted from the comparison algorithms between the demand current signals and feedback current signals [16]. A hysteresis band (HB) is used in the HC technique to determine the high or low level of switching pulse. In [17], the HC method with a fixed-HB is applied to control the IMD. IMD controlled by the HC method worked stably with a periodic rotor flux angle in various operating conditions. In [18], the speed control of IMD applying the HC method is performed with various HB values. The high performance of IMD is demonstrated by experiment results using DSP1103. Paper [19] describes two HC methods corresponding to fixed-HB and sinusoidal-HB for speed control of IMD. The sinusoidal-HC method is more efficient and produces lower current harmonics than the fixed-HB method. Paper [20] presents three HC types: fixed-HB, variable-HB, and fuzzy-HB. The simulation results have proved that the Fuzzy-HC process has the best effect on ripple and harmonics.

In typical SPWM, the inverter switching pulses are generated from comparing the demand three-phase voltages signals and high-frequency triangular carrier waves [16, 21]. The

modulation method works effectively when the amplitude of the sinusoidal modulation wave is less or equal than that of the carrier wave [22]. The paper [23] presents a control model of IMD using SPWM with an improving speed control unit. The sliding mode control technique is applied to the speed controller instead of the classical PI technique in this article.

Both the HC and SPWM methods have the same FOC control schemes. Because the inverter switching control is directly controlled by current, the HC method has a lower overshoot during transient states. On the other hand, the SPWM method has the advantage of lower ripple in operation. In this paper, the HCSPWM method combining HC and SPWM techniques is proposed for speed control in IMDs. The proposed method combines the advantages of the above two ways in the motor control process, including low overshoot in the transient phase and low ripple in the steady phase. The simulations are performed at nominal speed and low speeds to prove the efficiency of the proposed method.

2. The FOC method for speed control in IMD

Three motor speed control methods, including HC, SPWM, and HCSPWM, will be presented in this section.

2.1. The FOC scheme applying the HC control technique

The block diagram of the IMD applying the HC technique for the speed control is illustrated in Fig. 2. Reference values, including magnetizing current and motor speed, are set for the operating mode of the IMD. The measured stator currents and rotor speed are feedback to the controller using the FOC scheme.

The three-phase stator current is transformed into $[\alpha, \beta]$ coordinate by Clarke, as Eq. (1):

$$\begin{bmatrix} i_\alpha \\ i_\beta \end{bmatrix} = \begin{bmatrix} \frac{2}{3} & -\frac{1}{3} & -\frac{1}{3} \\ 0 & \frac{1}{\sqrt{3}} & -\frac{1}{\sqrt{3}} \end{bmatrix} \times \begin{bmatrix} i_a \\ i_b \\ i_c \end{bmatrix} \quad (1)$$

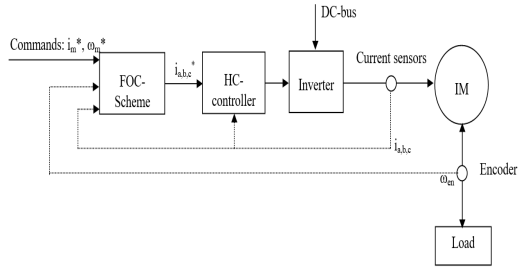

(a) General Block diagram

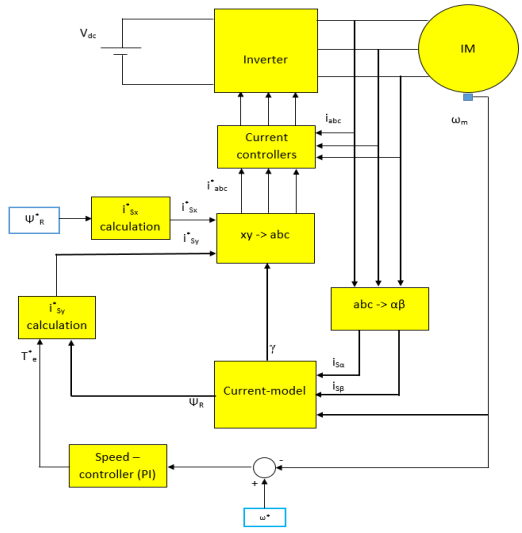

(b) Detailed block diagram

Fig. 2: Block diagram of the FOC using HC control [17]. Three-phase current is converted from $[a, b, c]$.

Where three-phase current "i_a, i_b, i_c" can be measured directly, or we can also measure two currents "i_a, i_b" and determine "i_c" by the Kirchoff law: $i_c = -i_a - i_b$.

In the Current model block [17], current elements "i_{Sd}, i_{Sq}" in rotating coordinate corresponding to rotor axis are transformed from currents in $[\alpha, \beta]$ coordinate, as Eq. (2):

$$\begin{bmatrix} i_{Sd} \\ i_{Sq} \end{bmatrix} = \begin{bmatrix} \cos\varepsilon & \sin\varepsilon \\ -\sin\varepsilon & \cos\varepsilon \end{bmatrix} \times \begin{bmatrix} i_{S\alpha} \\ i_{S\beta} \end{bmatrix} \quad (2)$$

$$\varepsilon = \int p\omega_m dt$$

The current elements "$i_{md,q}$" are calculated by Eq. (3):

$$i_{md,q} = \frac{1}{T_R s + 1} i_{Sd,q} \quad (3)$$

In Eqs. (4), (5), magnetizing current elements in $[\alpha, \beta]$ system are converted to determine the rotor flux vector in the Current-model, as in Fig. 2 and Fig. 3.

$$\begin{bmatrix} i_{m\alpha} \\ i_{m\beta} \end{bmatrix} = \begin{bmatrix} \cos\varepsilon & -\sin\varepsilon \\ \sin\varepsilon & \cos\varepsilon \end{bmatrix} \times \begin{bmatrix} i_{md} \\ i_{mq} \end{bmatrix} \quad (4)$$

$$\begin{cases} \text{- Amplitude of magnetizing current:} \\ i_m = \sqrt{(i_{m\alpha}^2 + i_{m\beta}^2)} \\ \text{- Amplitude of the rotor flux: } \psi_R = L_m i_m \\ \text{- Angle of the rotor flux: } \gamma = arctg(\frac{i_{m\beta}}{i_{m\alpha}}) \end{cases} \quad (5)$$

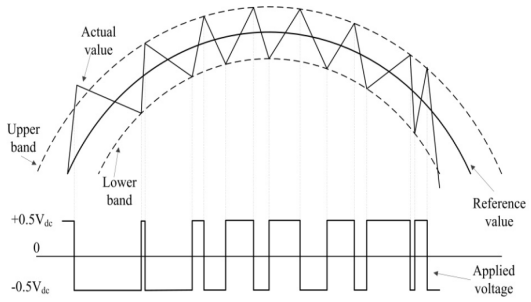

Fig. 3: Hysteresis current control technique [19].

As a result, with the input of current components "$i_{s\alpha}, i_{s\beta}$" through Eqs from (2) to (4), the current model has estimated the magnitude and angle of the rotor flux.

Through the ideal PI controller, the deviation between the feedback rotor speed and the reference speed is estimated by the adaptation algorithm as below:

$$Y = K_p[X(e) + K_i \int_0^t X(e)dt] \quad (6)$$

where $Y = T_e^*; X(e) = \omega(e); \omega(e) = \omega^* - \omega_m$.

The reference current elements "i_{Sx}, i_{Sy}" are determined from the setting value and measured rotor speed value, as in Eq. (7), (8).

$$i_{Sx}^* = i_m^* \quad (7)$$

$$i_{Sy}^* = \frac{2}{3p} \times \frac{L_R T_e^*}{L_m \psi_R} \quad (8)$$

The reference three-phase stator current "i_a^*, i_b^*, i_c^*" is converted as Eq. (9).

$$\begin{bmatrix} i_a^* \\ i_b^* \\ i_c^* \end{bmatrix} = \begin{bmatrix} \cos(\gamma) & -\sin(\gamma) \\ \cos(\gamma - \frac{2\pi}{3}) & -\sin(\gamma - \frac{2\pi}{3}) \\ \cos(\gamma + \frac{2\pi}{3}) & -\sin(\gamma + \frac{2\pi}{3}) \end{bmatrix} \times \begin{bmatrix} i_{Sx}^* \\ i_{Sy}^* \end{bmatrix} \quad (9)$$

The actual three-phase current is compared with the reference three-phase current to generate the inverter switching pulses. As a result, the actual current will be maintained inside the boundary corresponding to the hysteresis band as Fig. 3, [19].

2.2. The FOC scheme applying the SPWM technique

In this case, the FOC unit will provide the reference voltage as output signals for the SPWM controller to generate the inverter switching pulses. The block diagram of IMD applying the SPWM technique for the speed control is illustrated in Fig. 4.

In the block "T2/3," the three-phase stator current is converted into $[\alpha, \beta]$ coordinate by Eq. (1).

Like the HC control technique, the Current-model is used to generate magnetizing current "i_m," and the rotor flux angle "γ," by Eqs. (2)-(5).

In the block "T2/2," the actual current in $[\alpha, \beta]$ combined with the rotor flux angle to transfer into $[x, y]$ coordinate system, as below:

$$\begin{bmatrix} i_{sx} \\ i_{sy} \end{bmatrix} = \begin{bmatrix} \cos\gamma & \sin\gamma \\ -\sin\gamma & \cos\gamma \end{bmatrix} \times \begin{bmatrix} i_\alpha \\ i_\beta \end{bmatrix} \quad (10)$$

By applying the PI controller, as in Eq. (6), the difference between the setting and actual magnetizing current is used to create the reference current component "i_{Sx}^*." And, the difference between reference speed and measured speed is used to generate the reference current component "i_{Sy}^*."

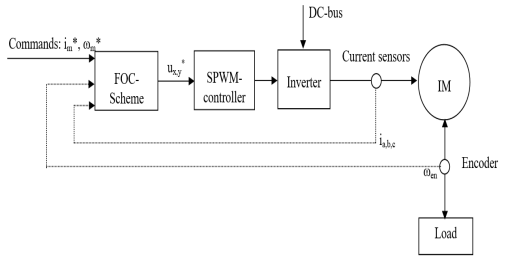

(a) General Block diagram

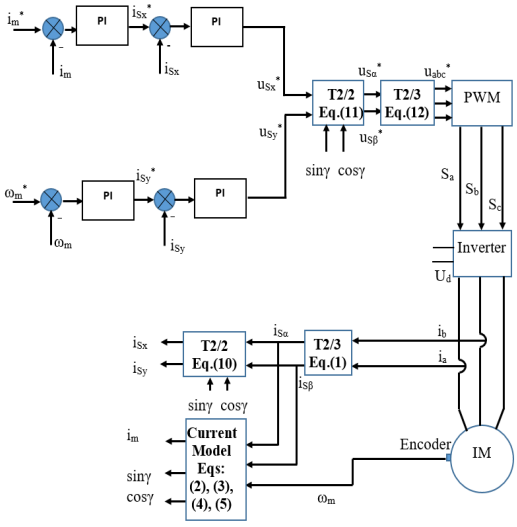

(b) Detailed block diagram

Fig. 4: Block diagram of the FOC using SPWM technique.

In the $[x, y]$ coordinate system, the difference between the reference current and the actual current through the PI controller will generate the reference voltage, "u_{Sx}^*, u_{Sy}^*."

The voltage signals in $[x, y]$ coordinate are inversely converted into $[\alpha, \beta]$ by Eq. (11):

$$\begin{bmatrix} u_{S\alpha} \\ u_{S\beta} \end{bmatrix} = \begin{bmatrix} \cos\gamma & -\sin\gamma \\ \sin\gamma & \cos\gamma \end{bmatrix} \times \begin{bmatrix} u_{Sx} \\ u_{Sy} \end{bmatrix} \quad (11)$$

The voltage signals in $[\alpha, \beta]$ coordinate are inversely converted into $[a, b, c]$ by Eq. (12):

$$\begin{bmatrix} u_a^* \\ u_b^* \\ u_c^* \end{bmatrix} = \begin{bmatrix} 1 & 0 \\ -\frac{1}{2} & \frac{\sqrt{3}}{2} \\ -\frac{1}{2} & -\frac{\sqrt{3}}{2} \end{bmatrix} \times \begin{bmatrix} u_{S\alpha}^* \\ u_{S\beta}^* \end{bmatrix} \quad (12)$$

The reference voltage signals are modulated by the SPWM technique [24], as in Fig. 5, to generate the inverter switching pulses for speed control in IMD.

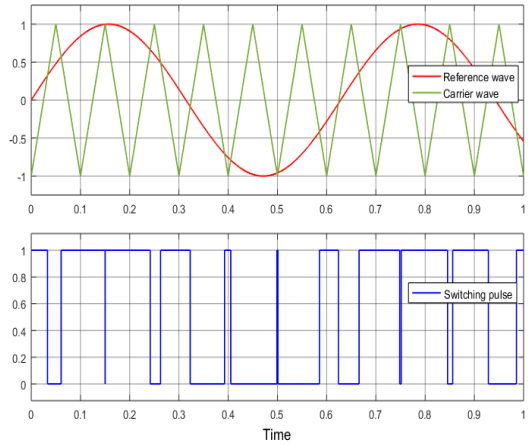

Fig. 5: Typical SPWM technique.

2.3. The FOC scheme applying the HCSPWM technique

Because both the HC and SPWM techniques use the FOC control scheme, two control methods can be designed to operate parallel. A method combining HB control with SPWM control by the OR logical operator, called the HCSPWM method, is proposed to generate the inverter switching pulses. The control structure of the HCSPWM method is shown in Fig. 6.

Similar to the two above control structures, the measured current "i_a, i_b" are transformed into $[\alpha, \beta]$ and $[x, y]$ coordinate systems. The current model is used to estimate the magnetizing current, rotor flux components.

Two control methods, including HC and SPWM, operate parallel, as described in Fig. 6-(b), with corresponding equations.

Figures 7 and 8 describe the combination of HC and SPWM methods for generating switching pulses for inverter control in the proposed method.

IMD applying method HCSPWM has the advantages of both methods HC and SPWM. The

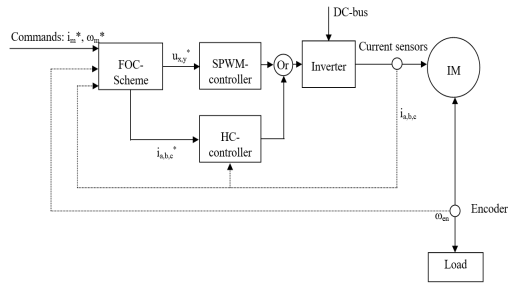

(a) General Block diagram

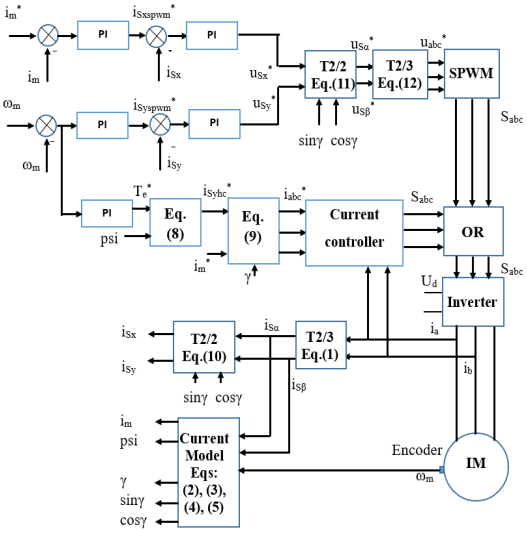

(b) Detailed block diagram

Fig. 6: Block diagram of the FOC using HCSPWM technique.

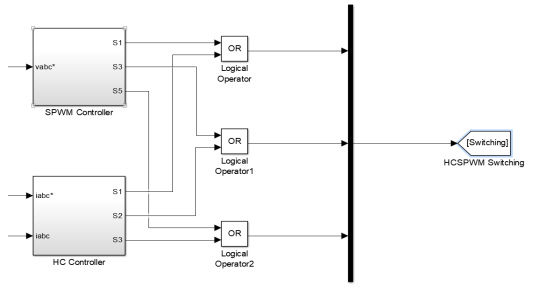

Fig. 7: Switching pulse generation of HCSPWM technique.

control response has a lower overshoot in the transient phase and a lower ripple during the steady operation phase.

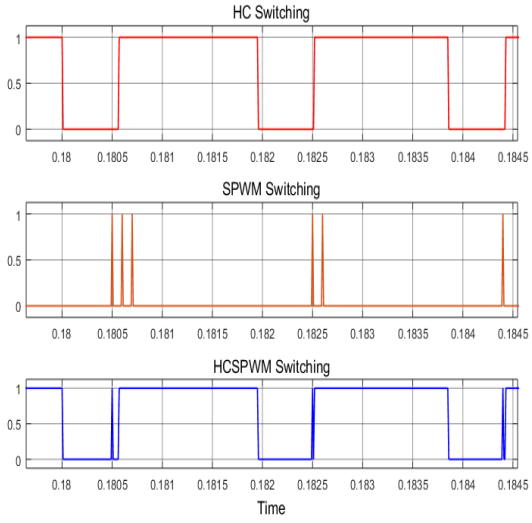

Fig. 8: Switching pulses of HC, SPWM, HCSPWM technique.

3. Simulation results

Speed control simulations of IMD will be performed corresponding to three above control method in MATLAB/SIMULINK environment. The motor parameters are listed as below:

P_{rated}= 2.2 (kW), ω_{rated} = 1420 (rpm),

U_{rated} = 400 (V), p = 2, $T_{rated\,load}$ = 14.8 (Nm)

R_S = 3.179 (Ω), R_R = 2.118 (Ω),

L_S = 0.209 (H), L_R = 0.209 (H), L_m = 0.192 (H)

The FOC structure model in MATLAB/SIMULINK is implemented according to the block diagram in Fig. 6-(b). Simulations will be implemented with each method in order under various operating conditions.

Integral Time Absolute Error (ITAE) index is used for assessing each method's performance [25]. The ITAE index is appropriate for evaluating the error between an actual signal and a reference signal in the steady-state for a long time. In this paper, the IATE index is estimated

for 5 seconds.

$$ITAE = \int_0^T t\,|e_\omega(t)|\,dt \tag{13}$$

where $e_\omega(t) = \omega_{en} - \omega_m^*$.

Total harmonic distortion of the current (THDI) index is used for assessing the quality of the phase current [26, 27], as shown below:

$$THDI(\%) = \sqrt{\frac{\sum_{n=2}^{\infty} I_n^2}{I_1^2}}100 \tag{14}$$

Where: "I_1" RMS value of fundamental frequency current; "I_n," RMS value of harmonic frequency current; n: harmonic order.

Study 1: The performance of the IMD system is simulated at a reference speed of 1000 rpm with a load of 10 Nm in three methods according to the sequence HC, SPWM, HCSPWM methods. The demand speed is set from zero to rated speed in 0.5 seconds, with a rated load value and the simulation process corresponding to T=1.5 s.

Figures 9-(a), 10-(a), and 11-(a) present the real speed responses of three control methods in speed control of IMD. The overshoot of the SPWM method is the highest of the three methods. Otherwise, the proposed HCSPWM method has an overshoot equivalent to the HC method.

The three-phase currents are depicted in parts: b) of Figs. 9-11. In the steady-state, the stator current in the HC method has the highest harmonic of the three methods. Parts c) shows the presentative switching pulse period of three methods. Parts d) of Figs. 9-11 present the electrical torque of the methods. The electrical torque of the HC method oscillates very vigorously; in contrast, the other two methods have a slight fluctuation.

The overshoot speed, total harmonic distortion current (THDI), and ITAE index of the methods are present in Tab. 1. The HCSPWM method combines the advantages of the HC and SPWM methods with low overshoot, small ripple, and low harmonic distortion. The proposed method has an overshoot similar to the HC control method in the transient phase. Besides, the IMD operates for a long time, the ITAE, the THDI indexes of the HCSPWM method will be equivalent to that of the SPWM method.

Tab. 1: Overshoot speed, ITAE index, THDI of three control methods at 1000 rpm – 10 Nm.

	HC	SPWM	HCSPWM
Overshoot (rpm)	8	36	12
ITAE index	0.6974	0.4761	0.5768
THDI(%)	11.25	1.2	1.2

Study 2. Like the above case, the speed control is simulated at a reference speed of 355 rpm (25% rated speed) with a load of 3 Nm. The motor accelerates quickly and reaches a steady-state corresponding to the command speed, as in Figs. 12-(a), 13-(a), and 14-(a).

The overshoot of the SPWM method is still the highest of the three methods in this case. The proposed HCSPWM method has an equivalent overshoot with the HC method. In the steady-state, the stator current is most distorted in the HC method. The HCSPWM method has the same current distortion as the steady-state SPWM method, as in Parts b) of Figs. 12-14. The switching pulse of the three methods is described in Parts c). The electrical torque is indicated in Figs. 12-(d), 13-(d), and 14-(d). The overshoot speed, total harmonic distortion current, and ITAE index are present in Tab. 2.

Tab. 2: Overshoot speed, ITAE index, THDI of three control methods at 355 rpm – 3 Nm.

	HC	SPWM	HCSPWM
Overshoot (rpm)	4	14	6
ITAE index	0.3069	0.237	0.239
THDI(%)	7.4	1.5	1.8

Study 3: Similar to the above case, the speed control is simulated at a reference speed of 5% rated speed (71 rpm) with a load of 3 Nm. The motor accelerates quickly and reaches a steady-state corresponding to the command speed, as in Figs. 15-(a), 16-(a), and 17-(a).

The SPWM method still has the highest overshoot of the simulation methods. The proposed HCSPWM method has an overshoot similar to the HC method. The HCSPWM method has the same current distortion as the SPWM method in the steady-state, as shown in Parts b) of Figs. 15-17. Parts c) present the switching pulse diagram of three techniques. In the steady-state, the stator current is most distorted in the HC method. The electrical torque is shown in Figs. 15-(d), 16-(d), and 17-(d). The overshoot speed, total harmonic distortion current, and ITAE index are present in Tab. 3.

Tab. 3: Overshoot speed, ITAE index, THDI of three control methods at 71 rpm – 3 Nm.

	HC	SPWM	HCSPWM
Overshoot (rpm)	0.5	2	0.8
ITAE index	0.2512	0.1166	0.1199
THDI(%)	8.7	1.1	1.1

The simulation results demonstrated that the proposed method has a fast control response with low overshoot during transient and low ripple in steady operation. The specific of the proposed method combines the advantages of each component technique with each appropriate control stage. The HCSPWM method can be considered equivalent to a soft-switching strategy between two control structures corresponding to two operating stages while still maintaining the stability and synchronization of the IMD system.

4. Conclusion

The paper has proposed the HCSPWM method, combined from the HC and SPWM control techniques by the OR logical algorithm, according to the FOC schema for the speed control. The feasibility of the proposed method has been demonstrated through simulation results under various operating conditions. The proposed method obtained a lower overshoot than the SPWM method in the transient phase and a lower ripple than the HC method in the steady phase. In particular, the proposed method has an IATE index equivalent to the SPWM method in the steady-state of operation. The proposed method com-

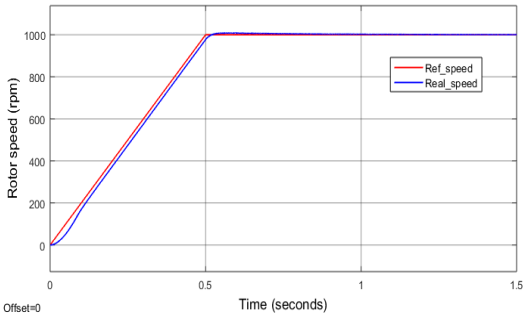

(a) Reference and real rotor speed

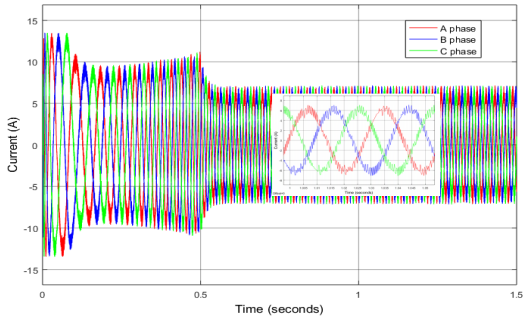

(b) Three-phase measured current

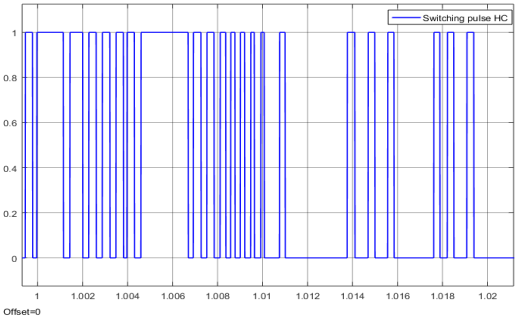

(c) Switching pulses

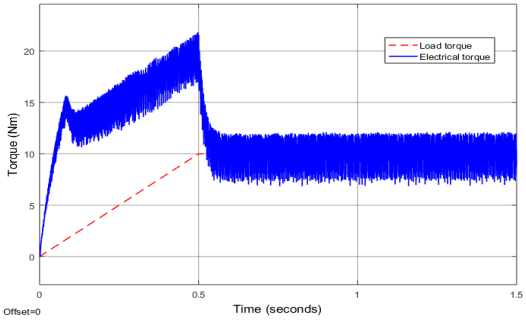

(d) Electrical torque

Fig. 9: FOC Performance with HC technique at 1000 rpm - 10 Nm.

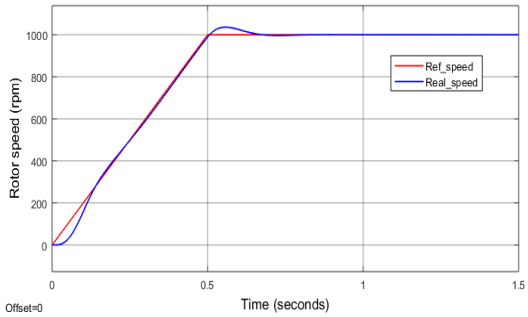

(a) Reference and real rotor speed

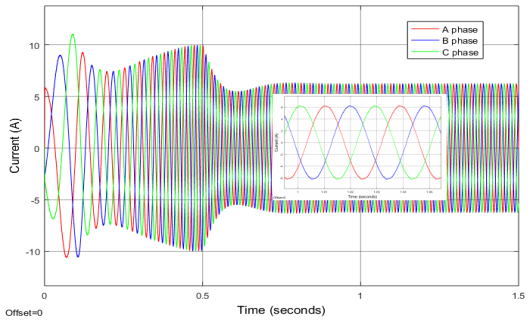

(b) Three-phase measured current

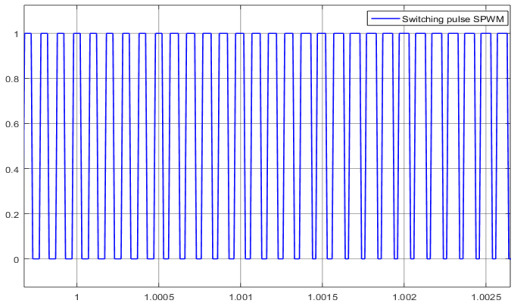

(c) Switching pulses

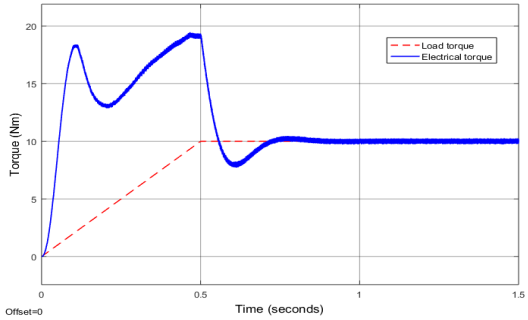

(d) Electrical torque

Fig. 10: FOC Performance with SPWM technique at 1000 rpm -10 Nm.

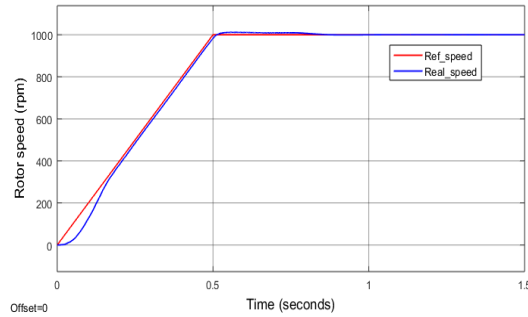

(a) Reference and real rotor speed

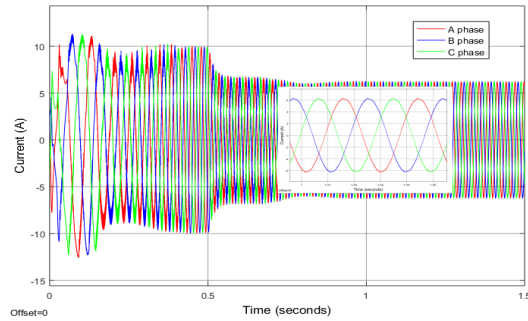

(b) Three-phase measured current

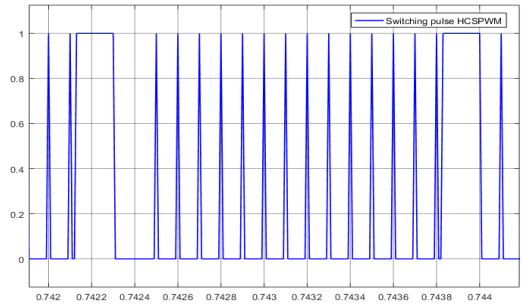

(c) Switching pulses

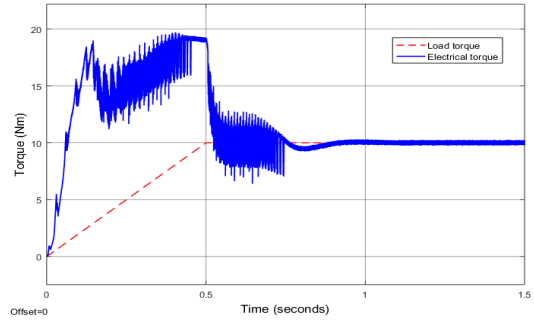

(d) Electrical torque

Fig. 11: FOC Performance with HCSPWM technique at 1000 rpm -10 Nm.

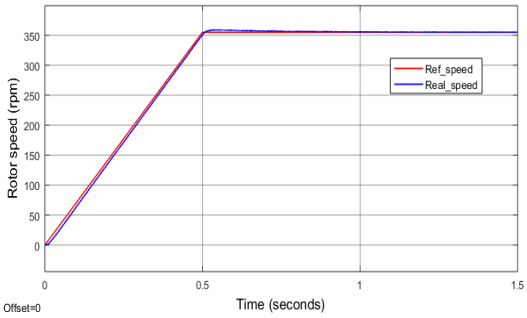

(a) Reference and real rotor speed

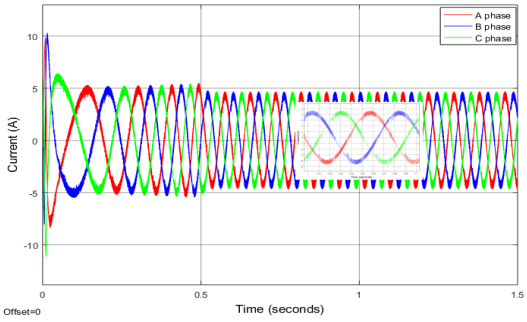

(b) Three-phase measured current

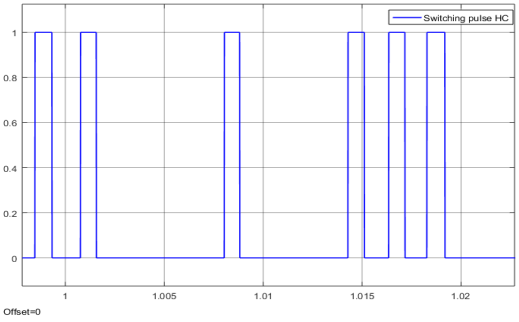

(c) Switching pulses

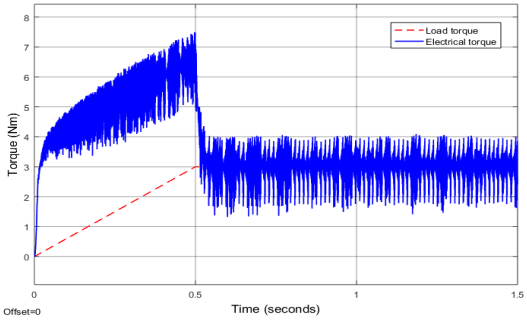

(d) Electrical torque

Fig. 12: FOC Performance with HC technique at 355 rpm – 3 Nm.

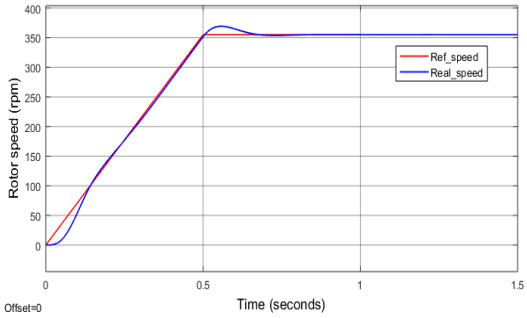

(a) Reference and real rotor speed

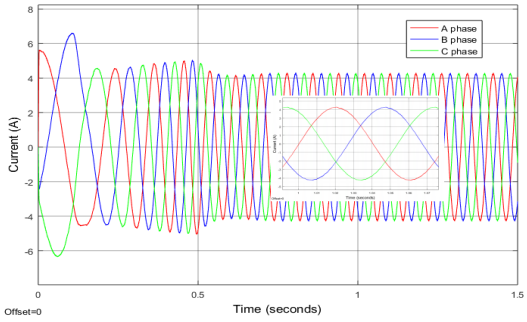

(b) Three-phase measured current

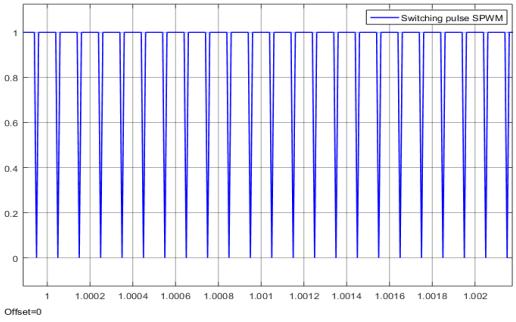

(c) Switching pulses

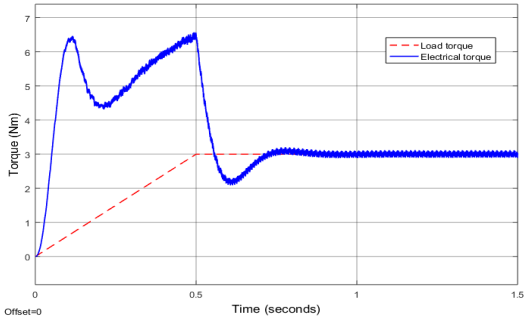

(d) Electrical torque

Fig. 13: FOC Performance with SPWM technique at 355 rpm – 3 Nm.

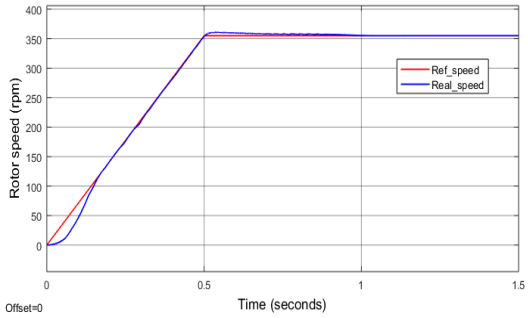

(a) Reference and real rotor speed

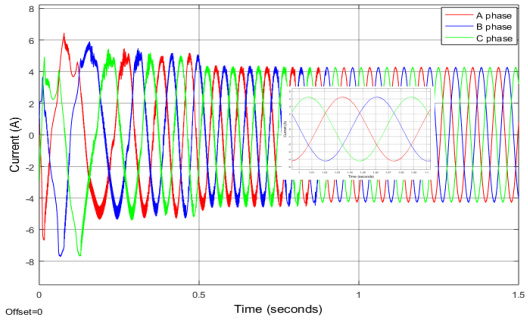

(b) Three-phase measured current

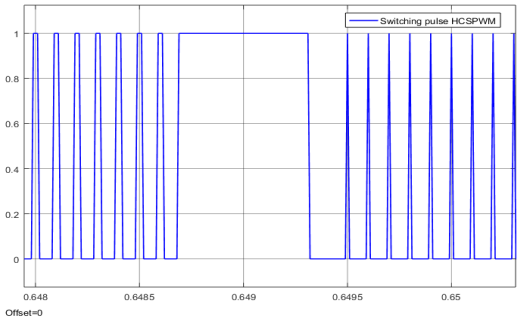

(c) Switching pulses

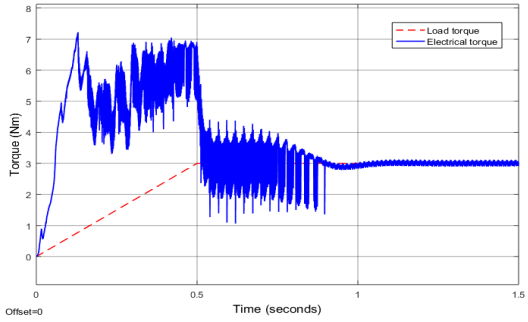

(d) Electrical torque

Fig. 14: FOC Performance with HCSPWM technique at 355 rpm – 3 Nm.

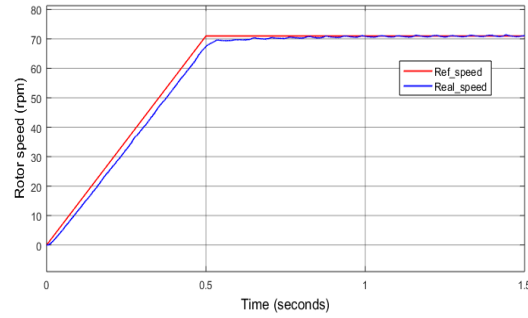

(a) Reference and real rotor speed

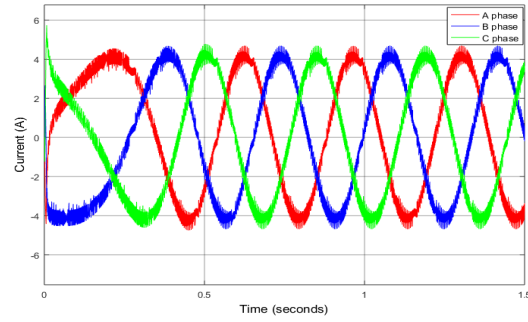

(b) Three-phase measured current

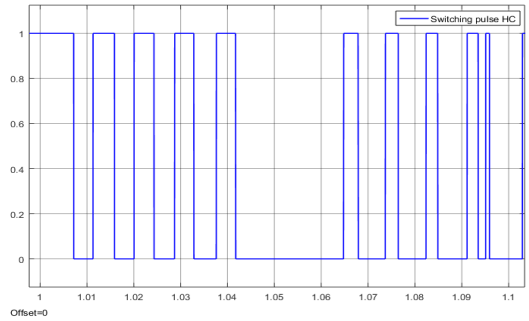

(c) Switching pulses

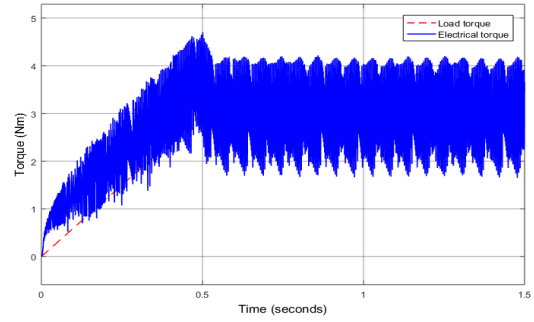

(d) Electrical torque

Fig. 15: FOC Performance with HC technique at 71 rpm – 3 Nm.

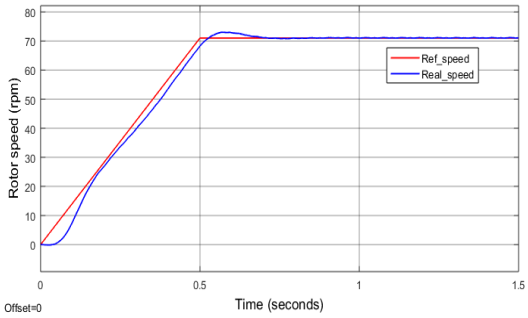

(a) Reference and real rotor speed

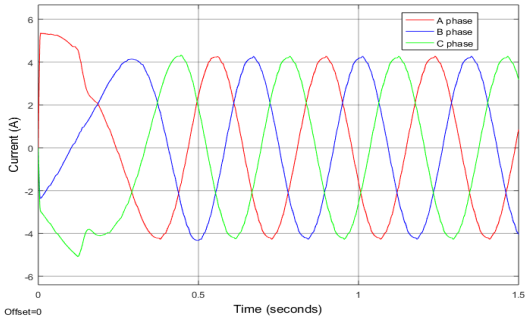

(b) Three-phase measured current

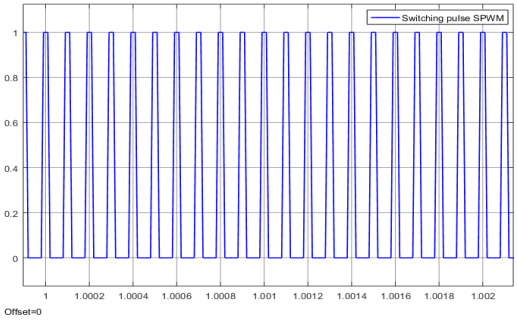

(c) Switching pulses

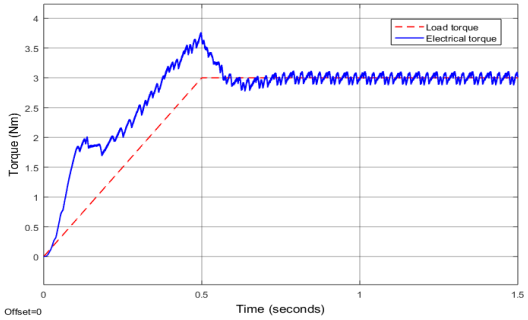

(d) Electrical torque

Fig. 16: FOC Performance with SPWM technique at 71 rpm – 3 Nm.

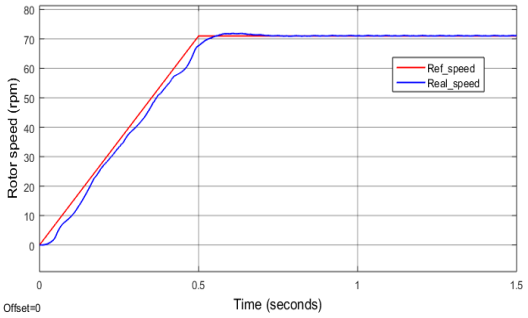

(a) Reference and real rotor speed

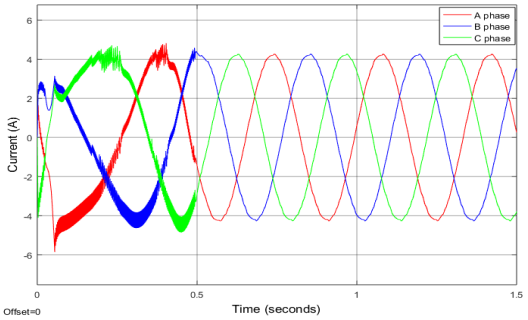

(b) Three-phase measured current

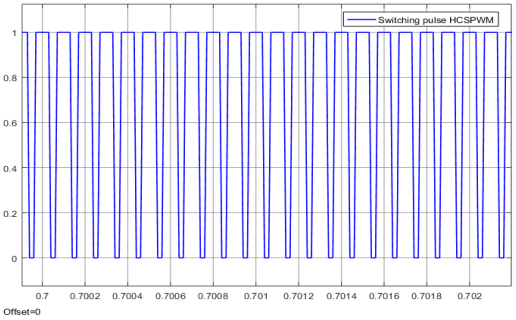

(c) Switching pulses

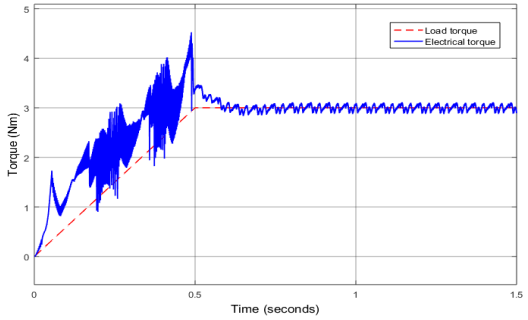

(d) Electrical torque

Fig. 17: FOC Performance with HCSPWM technique at 71 rpm – 3 Nm.

bined the advantages of each component method corresponding to the appropriate control stage. Thus, the HCSPWM method can be considered a possible selection in controlling the speed of the IMD. However, the proposed method is a mixed-method, so the high fluctuation in the starting phase still exists as a disadvantage of the HCSPWM method. Future studies should improve this problem by applying intelligent algorithms to adjust the PI controller's parameters and the hysteresis band to achieve a more efficient control process.

References

[1] Chan, T. F., & Shi, K. (2011). Applied intelligent control of induction motor drives. *John Wiley & Sons*.

[2] Vladimir, P., & Dmitry, S. (2018, March). To issue of designing scalar closed-loop controllers for frequency controlled induction motor drives. *In 2018 17th International Ural Conference on AC Electric Drives (ACED) (pp. 1-4). IEEE.*

[3] Karthik, D., & Chelliah, T. R. (2016, May). Analysis of scalar and vector control based efficiency-optimized induction motors subjected to inverter and sensor faults. *In 2016 International Conference on Advanced Communication Control and Computing Technologies (ICACCCT) (pp. 462-466). IEEE.*

[4] Travieso-Torres, J. C., Vilaragut-Llanes, M., Costa-Montiel, Á., Duarte-Mermoud, M. A., Aguila-Camacho, N., Contreras-Jara, C., & Álvarez-Gracia, A. (2020). New Adaptive High Starting Torque Scalar Control Scheme for Induction Motors Based on Passivity. *Energies*, 13(5), 1276.

[5] Verma, P., Saxena, R., Chitra, A., & Sultana, R. (2017, September). Implementing fuzzy PI scalar control of induction motor. *In 2017 IEEE International Conference on Power, Control, Signals and Instrumentation Engineering (ICPCSI) (pp. 1674-1678). IEEE.*

[6] Kohlrusz, G., & Fodor, D. (2011). Comparison of scalar and vector control strategies of induction motors. *Hungarian Journal of Industry and Chemistry*, 39(2), 265-270.

[7] Carlos Traviesotorres, J., Contreras-Jara, C., Diaz, M., Aguila-Camacho, N., & Duarte-Mermoud, M. (2021). New Adaptive Starting Scalar Control Scheme for Induction Motor Variable Speed Drives. *IEEE Transactions on Energy Conversion.*

[8] Dittrich, J. A., & Nguyen, P. Q. (2008). Vector control of three-phase AC machines: system development in the practice. Springer.

[9] Hill, R. J. (1994). Electric railway traction. II. Traction drives with three-phase induction motors. *Power Engineering Journal*, 8(3), 143-152.

[10] Vas, P. (1998). Sensorless vector and direct torque control.

[11] Mon-Nzongo, D. L., Jin, T., Ekemb, G., & Bitjoka, L. (2017). Decoupling network of field-oriented control in variable-frequency drives. *IEEE Transactions on Industrial Electronics*, 64(7), 5746-5750.

[12] Sirikan, P., & Charumit, C. (2020). Implementation of indirect rotor field oriented control for three phase induction motor drive based on TMS320F28335 DSP. *Przegląd Elektrotechniczny*, 96.

[13] Ho, S. D., Brandstetter, P., Palacky, P., Kuchar, M., Dinh, B. H., & Tran, C. D. (2021). Current sensorless method based on field-oriented control in induction motor drive. *Journal of Electrical Systems*, 17(1).

[14] Kumar, A., & Ramesh, T. (2015, May). Direct field oriented control of induction motor drive. *In 2015 Second International Conference on Advances in Computing and Communication Engineering (pp. 219-223). IEEE.*

[15] Li, W., Xu, Z., & Zhang, Y. (2019, May). Induction motor control system based on FOC algorithm. *In 2019 IEEE 8th Joint International Information Technology and*

Artificial Intelligence Conference (ITAIC) (pp. 1544-1548). IEEE.

[16] Banerjee, T., Bera, J. N., Chowdhuri, S., & Sarkar, G. (2016, January). A comparative study between different modulations techniques used in field oriented control induction motor drive. *In 2016 2nd International Conference on Control, Instrumentation, Energy & Communication (CIEC) (pp. 358-362). IEEE.*

[17] Tran, C. D., Brandstetter, P., Dinh, B. H., & Dong, C. S. T. (2021). An Improving Hysteresis Current Control Method Based on FOC Technique for Induction Motor Drive. *Journal of Advanced Engineering and Computation*, 5(2), 83-92.

[18] Talib, M. H. N., Isa, S. M., Hamidon, H. E., Ibrahim, Z., & Rasin, Z. (2016, November). Hysteresis current control of induction motor drives using dSPACE DSP controller. *In 2016 IEEE International Conference on Power and Energy (PECon) (pp. 522-527). IEEE.*

[19] Zhang, J., Li, L., Zhang, L., & Dorrell, D. G. (2017, October). Hysteresis band current controller based field-oriented control for an induction motor driven by a direct matrix converter. *In IECON 2017-43rd Annual Conference of the IEEE Industrial Electronics Society (pp. 4633-4638). IEEE.*

[20] Farah, N., Talib, M. H. N., Ibrahim, Z., Isa, S. M., & Lazi, J. M. (2017, October). Variable hysteresis current controller with fuzzy logic controller based induction motor drives. *In 2017 7th IEEE International Conference on System Engineering and Technology (ICSET) (pp. 122-127). IEEE.*

[21] Jena, S. P., & Rout, K. C. (2018, May). Comparative analysis of harmonic reduction of VSI fed induction motor using SVPWM and sinusoidal PWM. *In 2018 2nd International Conference on Trends in Electronics and Informatics (ICOEI) (pp. 1-5). IEEE.*

[22] Kabashi, Q., Limani, M., Caka, N., & Zabeli, M. (2018). Low Order Harmonic Analysis of 3-Phase SPWM and SV-PWM Inverter Systems Driving an Unbalanced 3-Phase Induction Motor Load. *Modelling and Simulations (IREMOS)*, 134.

[23] Mahfoud, S., Derouich, A., El Ouanjli, N., Mohammed, T., & Hanafi, A. (2021). Field Oriented Control of Doubly Fed Induction Motor using Speed Sliding Mode Controller. *In E3S Web of Conferences (Vol. 229, p. 01061). EDP Sciences.*

[24] Kim, S. H. (2017). Electric motor control: DC, AC, and BLDC motors. Elsevier.

[25] Shuaib, A. O., & Ahmed, M. M. (2014). Robust PID control system design using ITAE performance index (DC motor model). *International Journal of Innovative Research in Science, Engineering and Technology*, 3(8), 15060-15067.

[26] Sousa, V., Hernández, H., Quispe, E. C., Gómez, J. R., & Viego, P. R. (2017, May). Analysis of harmonic distortion generated by PWM motor drives. *In 2017 IEEE Workshop on Power Electronics and Power Quality Applications (PEPQA) (pp. 1-6). IEEE.*

[27] IEEE Recommended Practice and Requirements for Harmonic Control in Electric Power Systems (IEEE Std 519-2014)

About Authors

Minh TRAN was born in Vietnam in 1985. He has a Ph.D. degree in Electrical Engineering. Now, he is a lecturer at the Faculty of Electrical and Electronics Engineering at Ton Duc Thang University, Ho Chi Minh City, Vietnam. His research interests are the application of modern control methods and intelligent algorithms in induction motor drives.

Cuong Dinh TRAN was born in Vietnam in 1982. He received a Ph.D. degree in Electrical Engineering from VSB-Technical University of Ostrava, Czech Republic, in 2020. Now, he is a lecturer at the Faculty of Electrical and Electronics Engineering at Ton Duc Thang

University, Ho Chi Minh City, Vietnam. he is a leader of the student research group on "modern control methods of AC machines." His research interests are the application of modern control methods and intelligent algorithms in induction motor drives.

Bach Hoang DINH received a Ph.D. degree in Electrical Engineering from Heriot-Watt University, Edinburgh, the United Kingdom, in 2009. He received the BE and ME degrees in Electrical Engineering from Vietnam National University - Hochiminh City in 1995 and 1998. Bach Dinh is currently the head of the Electrical Engineering Department, Faculty of Electrical and Electronics Engineering at Ton Duc Thang University. His research interests are intelligent and optimal control, computer vision, robotics, power electronics, SCADA, and industrial communication networks. He is a member of the IEEE Industrial Electronics Society.

Tai Thanh PHAN was born in Vietnam in 1995. He received a Master degree in Electrical Engineering from Ton Duc Thang University, Ho Chi Minh City, Vietnam, in 2020. Now, he is a lecturer at the Faculty of Electrical and Electronics Engineering at Ton Duc Thang University, Ho Chi Minh City, Vietnam. His research areas are the application of optimization algorithms in the power system, renewable energy, and control engineering.

Trang Huynh Cong NGUYEN was born in Vietnam in 2000. Now, he is a student at the Faculty of Electrical and Electronics Engineering at Ton Duc Thang University, Ho Chi Minh City, Vietnam. His research interests are the application of modern control methods and intelligent algorithms in induction motor drives. He is a member of the student research group on "modern control methods of AC machines."

Huy Truong NGUYEN was born in Vietnam in 2000. Now, he is a student at the Faculty of Faculty of Electrical and Electronics Engineering at Ton Duc Thang University, Ho Chi Minh City, Vietnam. His research interests are the application of modern control methods and intelligent algorithms in induction motor drives. He is a member of the student research group on "modern control methods of AC machines."

Giang Thi Tuyet LAI was born in Vietnam in 2002. Now, she is a student at the Faculty of Electrical and Electronics Engineering at Ton Duc Thang University, Ho Chi Minh City, Vietnam. Her research interests are the application of modern control methods and intelligent algorithms in induction motor drives. She is a member of the student research group on "modern control methods of AC machines."

Huy Xuan PHAN was born in Vietnam. He graduated from the University of Technology, Ho Chi Minh City, Viet Nam. He received his ME degrees in electrical – electronics power engineering. Now, he is working at Long An Power company, Long An province, Vietnam. His research interests include modern control methods of electrical drives, automatic control system, intelligent control system, operation and control power system.